

PREDICTING CONVECTIVE HEAT TRANSFER DURING UNSTEADY FLOW IN CUBIC PERIODIC OPEN CELLULAR STRUCTURES

Konrad Dubil^{1*}, Thomas Wetzel¹, Benjamin Dietrich¹

¹Institute of Thermal Process Engineering, Karlsruhe Institute of Technology, Karlsruhe, Germany

1. INTRODUCTION

Periodic open cellular structures (POCS) are innovative structured internals for heat transfer applications. They are of special interest as tailor-made components for apparatuses in compact cooling and heating systems due to their continuous fluid and solid phases as well as their large design freedom. In order to evaluate the potential of POCS and to enable an application-oriented design, a detailed knowledge of the relation between their geometry and heat transfer capability is necessary. This contribution focuses on the investigation of the convective heat transfer in POCS with cubic unit cells during unsteady laminar flow. Numerical simulations have been carried out with varying dimensionless longitudinal and transversal pitches ($s_L = s_T = 3; 4; 5$) as well as Reynolds numbers ($Re = 10 - 100$) identifying the transition from the steady to the unsteady laminar flow regime. Based on a superposition approach (see Figure 1), a physically founded model for the prediction of the heat transfer coefficient is developed. The results calculated by the model show an excellent agreement with the simulation data.

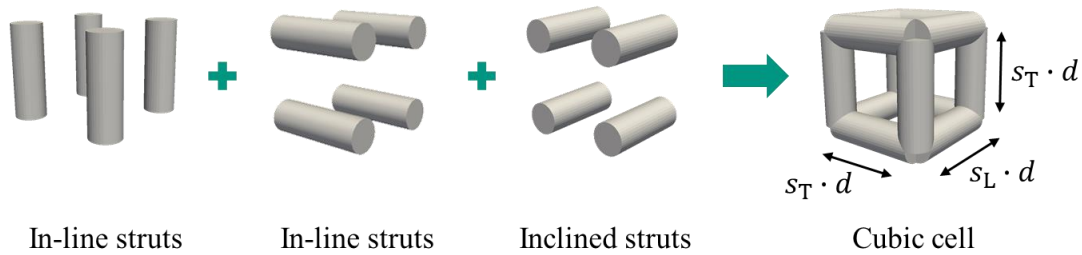


Figure 1: Scheme of the superposition approach and definition of longitudinal as well as transversal pitches.

2. NUMERICAL APPROACH

The numerical simulations were performed using the open source software OpenFOAM [1] (version 6), which discretizes the governing equations (conservation of mass, momentum and energy) with the finite volume method. During this work, the buoyantBoussinesqPimpleFoam solver was used in combination with the PISO algorithm and second order discretization schemes to calculate the unsteady incompressible flow fields in the porous structures. Buoyancy effects were neglected. Turbulence models were not needed due to the laminar flow regimes investigated. The working fluid was water with constant physical properties at 32 °C (see Table 1).

Table 1: Properties of water at 32 °C [2].

| Properties | Values |
|--|----------------------|
| Density $\rho_F / \frac{\text{kg}}{\text{m}^3}$ | 995 |
| Kinematic viscosity $\nu_F / \frac{\text{m}^2}{\text{s}}$ | $7.68 \cdot 10^{-7}$ |
| Specific heat capacity $c_{p,F} / \frac{\text{J}}{\text{kg}\cdot\text{K}}$ | 4180 |
| Thermal conductivity $k_F / \frac{\text{W}}{\text{m}\cdot\text{K}}$ | 0.617 |
| Prandtl number $Pr_F / -$ | 5.18 |

*Corresponding Author: konrad.dubil@kit.edu

To minimize the computational effort, the periodicity of the investigated structures was exploited. By implementing periodic boundary conditions based on the suggestions of Beale and Spalding [3], a simulation volume of two unit cells along each spatial direction was sufficient to obtain hydrodynamically and thermally developed flow fields. The size of the simulation volume can be considered representative of much larger structures, as preliminary studies have shown that increasing the volume does not alter the results. To estimate the discretization errors of the setup and the numerical grids, the so-called grid convergence index GCI was used as proposed by Roache [4]. The spatial and temporal resolutions resulted in GCI values below 2.1% and 0.05%, which was deemed as sufficiently low. Validation has been done by comparing the simulation results with data from literature, as shown in section 3.

3. RESULTS AND DISCUSSION

3.1 Boundaries of the unsteady laminar flow regime

Despite numerous publications investigating flow regimes in porous media, no comprehensive methodology exists to predict the regime boundaries [5]. Depending on the geometry of the porous medium, the transition from one regime to the other may occur at strongly varying Reynolds numbers. Therefore, the regime boundaries between the steady laminar and unsteady laminar as well as the beginning of the transitional regime have been identified for the cubic POCS investigated in this work. The onset of periodic vortices marked the end of the steady flow regime, whereas a strong broadening of the frequency spectrum corresponding to the evolution of chaotic wakes set the beginning of the transitional regime and the end of the unsteady laminar regime. The Reynolds number Re used in this work is defined according to Eq. (1) with d denoting the strut diameter, u_0 the superficial velocity, ψ the porosity of the structure and ν_F the kinematic viscosity of the fluid:

$$Re = \frac{u_0 \cdot L_c}{\psi \cdot \nu_F} \quad \text{with } L_c = \frac{\pi \cdot d}{2} \quad (1)$$

First, the beginning of the unsteady flow regime in in-line struts were compared with results from literature to check the numerical setup. Afterwards, the flow regime boundaries of cubic cells have been analysed. The results of both investigations are shown in Figure 2.

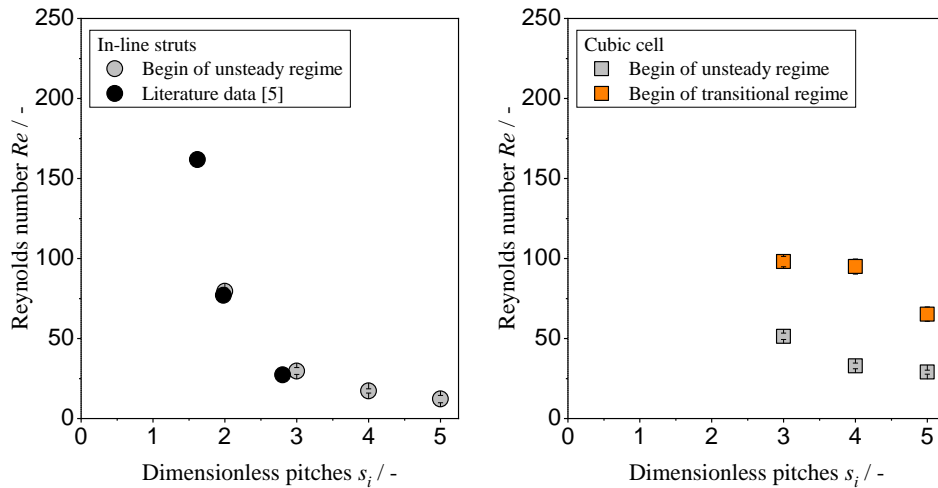


Figure 2: Reynolds numbers of in-line struts (left) and cubic cells (right) marking the transition between two flow regimes as a function of the dimensionless longitudinal pitch. The error bars indicate the respective upper and lower bounds of the corresponding flow regime transition. Additionally, data from Khalifa et al. is shown [5].

The simulation results agree well with the data provided by Khalifa et al. [5] supporting the validity of the setup. Both data sets indicate that a reduction of the dimensionless pitch postpones the onset of

the unsteady flow regime to higher Reynolds numbers. This is to be expected since a reduction of the free flow area increases the influence of viscous forces and thus stabilises the flow. The same explanation applies to the transition between steady to unsteady flow in cubic cells. They exhibit a similar curve progression to the in-line struts but the absolute Reynolds values are larger because of additional struts causing stabilisation of the flow. The beginning of the transitional regime also shifts to larger Reynolds numbers as the dimensionless pitch decreases. However, the curve progression is altered causing different sizes of the unsteady laminar flow regime for each cubic cell.

3.2 Analysis of the convective heat transfer

The results for the convective heat transfer are presented in terms of a time averaged non-dimensional Nusselt number Nu with h representing the heat transfer coefficient:

$$Nu = \frac{h \cdot L_c}{k_F} \quad \text{with } L_c = \frac{\pi \cdot d}{2} \quad (2)$$

The Nusselt number was determined for all cubic cells in a Reynolds range between $Re = 10 - 100$, except when the transitional flow regime was reached. The results are presented in Figure 3.

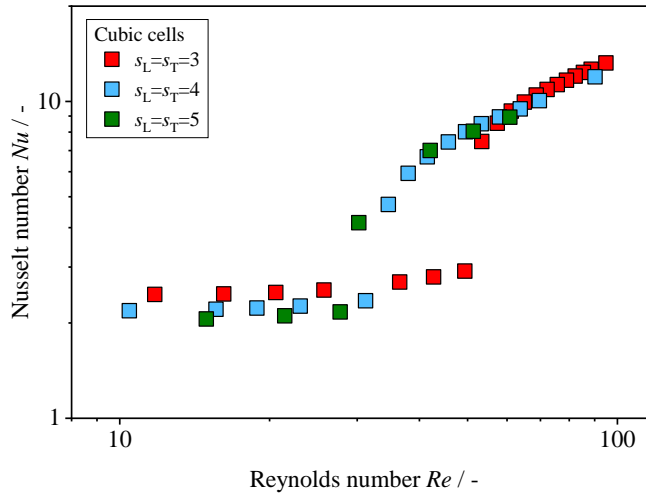


Figure 3: Nusselt numbers as a function of the Reynolds number for cubic cells with varying non-dimensional longitudinal and transversal pitches.

Two distinct curve progressions are observed: Sections with nearly constant Nusselt numbers and sections with positive slopes. In the first case, the flow fields of all structures remain steady and resemble flows through channels. Accordingly, the constant Nusselt numbers can be attributed to the steady state regime with undisturbed and fully developed thermal boundary layers [6; 7]. The latter sections coincide with the unsteady laminar flow regime. Vortices cause mixing of the flow and force a reformation of the thermal boundary layers leading to a change in the slope of the curve [6; 7]. Although the onset of vortex generation occurs at a defined Reynolds number, the resulting Nusselt number exhibits a gradual transition from the steady state to the unsteady flow regime. Apparently, the mixing capability of the vortices is initially not sufficient to cause a complete homogenisation of the temperature field in the fluid. However, as the Reynolds number increases, the temperature field approaches a homogenised state causing a full reformation of the thermal boundary layers.

For a first appraisal of the superposition approach (see Figure 1), the results obtained from cubic cells are compared to their corresponding in-line and inclined strut arrangements. Exemplarily, the Nusselt numbers of all three geometries with non-dimensional pitches of $s_L = s_T = 3$ are shown in Figure 4 as a function of the Reynolds number. A correlation for in-line struts developed by Gnielinski [8] is added to validate the results of the unsteady simulation cases (see Eq. (5)-(7)). As

shown in Figure 4, the in-line strut data fits the correlation fairly well in the fully developed unsteady flow regime with deviations of less than 20%.

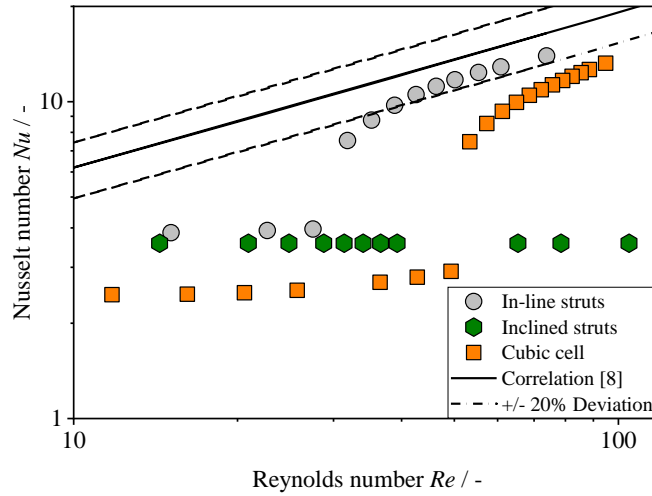


Figure 4: Nusselt numbers as a function of the Reynolds number for in-line struts, inclined struts and cubic cells with a non-dimensional longitudinal and transversal pitch of $s_L = s_T = 3$. Additionally, a correlation for in-line struts developed by Gnielinski [8] is shown.

The curve progression of the in-line struts resembles strongly that of the cubic cell. It has two distinct sections corresponding to the steady state and unsteady laminar flow regimes. However, the in-line struts show larger Nusselt numbers than the cubic cell over the entire investigated Reynolds range. This can be attributed to two effects. Near the junction of two struts in the cubic cell, the fluid flow stagnates reducing the local fluid velocity as well as the local heat transfer. Additionally, the contribution of the inclined struts to the overall heat transfer is significantly lower than that of the in-line strut arrangements reducing the average Nusselt number of the entire cubic cell. In contrast to the previously described geometries, the inclined struts remain in the steady state flow regime up to Reynolds numbers of 100. Due to the channel-like flow, the thermal boundary layers are fully developed leading to a constant Nusselt number. Therefore, the heat transfer is significantly reduced compared to the other two geometries in the unsteady laminar flow regime.

As stated above, the heat transfer within the cubic cells, which consist of in-line and inclined strut arrangements, appears to be influenced by both geometries. The cubic cells share several characteristics with the in-line struts, such as the curve progressions of the transition to the unsteady flow regime (see Figure 2) and the convective heat transfer (see Figure 4). However, the inclined struts postpone the beginning of vortex formation and reduce the overall heat transfer in the cell. Since these observations support the idea of superposition (see Figure 1), a corresponding modelling approach for the convective heat transfer is tested in section 3.3.

3.3 Modelling the convective heat transfer

The concept of superposition is used to model the convective heat transfer in cubic POCS during unsteady laminar flow. It is based on the idea that the interactions between the strut arrangements are negligibly small allowing the overall heat flux of the unit cell \dot{Q}_{cubic} to be described as the sum of the contributions of each strut arrangement with A denoting the surface area and ΔT the characteristic temperature difference:

$$\dot{Q}_{\text{cubic}} = \dot{Q}_{\text{in-line}} + \dot{Q}_{\text{inclined}} = (h_{\text{in-line}} \cdot A_{\text{in-line}} + h_{\text{inclined}} \cdot A_{\text{inclined}}) \cdot \Delta T \quad (3)$$

To account for the reduced heat transfer near the strut junctions (see section 3.2), a newly developed empirical factor is added, which reduces the respective surface area of the struts. After division by the

surface area of the cubic cell and the characteristic temperature difference, the Nusselt number of the cubic cell can be obtained from Eq. (4):

$$Nu_{\text{cubic}} = Nu_{\text{in-line}} \cdot \frac{2\pi \cdot d^2 \cdot (s_T - 1.29)}{A_{\text{cubic}}} + Nu_{\text{inclined}} \cdot \frac{\pi \cdot d^2 \cdot (s_L - 1.29)}{A_{\text{cubic}}} \quad (4)$$

For the use of the proposed equation, the convective heat transfer of the respective strut arrangements has to be known. As the heat transfer in in-line strut arrangements has been investigated by many authors for many years, multiple correlations are available for the range of Reynolds numbers of interest. In this work, a correlation developed by Gnielinski [8] is used to calculate the Nusselt number of the in-line struts with the Reynolds number proposed in section 3.1:

$$Nu_{\text{in-line}} = \left(0.3 + \sqrt{Nu_{\text{lam}}^2 + Nu_{\text{turb}}^2} \right) \cdot \left(1 + \frac{0.7 \frac{s_L}{s_T} - 0.3}{\left(1 - \frac{\pi}{4 \cdot s_T} \right)^{1.5} \left(\frac{s_L}{s_T} + 0.7 \right)^2} \right) \quad (5)$$

The correlation superimposes the contributions of the laminar heat transfer and turbulent heat transfer in the strut arrangements. The laminar Nusselt number Nu_{lam} is determined according to Eq. (6):

$$Nu_{\text{lam}} = 0.664 \cdot \sqrt{Re} \cdot \sqrt[3]{Pr} \quad (6)$$

The turbulent Nusselt number Nu_{turb} is obtained from Eq. (7):

$$Nu_{\text{turb}} = \frac{0.037 \cdot Re^{0.8} \cdot Pr}{1 + 2.443 \cdot Re^{-0.1} \cdot (Pr^{2/3} - 1)} \quad (7)$$

The convective heat transfer of the inclined struts is calculated according to Eq. (8), which was derived by fitting the simulation results obtained in this work.

$$Nu_{\text{inclined}} = \frac{9.3}{s_T} + 0.53 \quad (8)$$

Finally, the Nusselt numbers obtained from the simulations and Eq. (4) are compared in Figure 5.

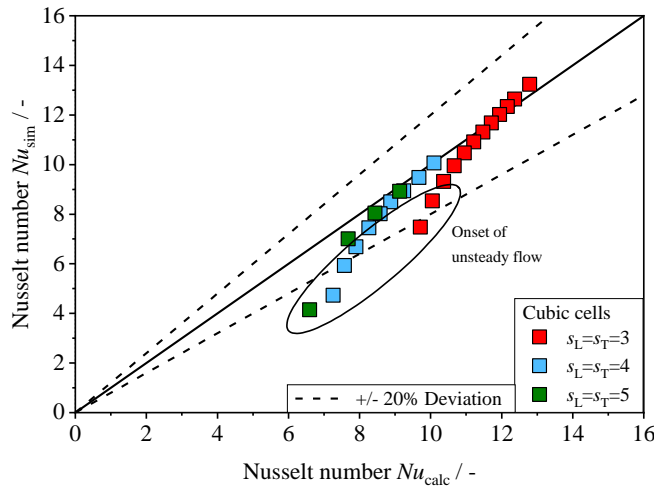


Figure 5: Comparison between the Nusselt numbers of cubic cells determined from numerical simulations in the unsteady laminar flow regime Nu_{sim} and the results obtained from the modelling approach developed in this work. The beginning of the unsteady flow regime is marked in the plot.

At the beginning of the unsteady laminar flow regime, larger discrepancies can be observed between the simulation results and the model. The gradual transition from the steady to the unsteady flow regime is not reflected by Gnielinski's correlation (see Figure 4) leading to a significant overestimation of the convective heat transfer. As stated by Žukauskas [9], the heat transfer at low Reynolds numbers may be affected by free convection increasing the determined Nusselt numbers in experimental data. Furthermore, Fowler and Bejan [10] pointed out that most experiments used for the derivation of the aforementioned correlations were conducted with a limited number of strut rows. According to their research, the results may still have been significantly influenced by entrance effects. In contrast, the numerical simulations neglect buoyancy effects as well as entrance effects due to the use of periodic boundary conditions. However, as the unsteady flow regime approaches a fully developed state in the simulations, a very good agreement between the simulation data and the model can be observed. The deviations become smaller than 5% showing the potential of this modelling approach.

4. CONCLUSIONS

The convective heat transfer in cubic POCS during unsteady laminar flow was investigated with numerical simulations. First, the regime boundaries were determined, which exhibit a pronounced dependency on the dimensionless pitch of the cubic cell. Afterwards, a strong influence of the present flow regime on the heat transfer coefficient was observed. Similarities between the characteristics of cubic cells and their corresponding in-line and inclined strut arrangements motivated the development of a new modelling approach. Based on the idea of superposition, a model for the prediction of the heat transfer coefficient in cubic POCS was developed, showing a very good agreement with the simulation results with a mean deviation of 18%.

ACKNOWLEDGEMENTS

The authors would like to thank the Friedrich und Elisabeth Boysen-Stiftung (BOY-145) for funding this work.

REFERENCES

- [1] H. G. Weller, G. Tabor, H. Jasak, C. Fureby, A tensorial approach to computational continuum mechanics using object-oriented techniques. *Computers in physics*, **12** (6) (1998) 620–631.
- [2] Verein Deutscher Ingenieure, VDI-Waermeatlas, Springer Vieweg, Berlin, Heidelberg (2013).
- [3] S. B. Beale, D. B. Spalding, Numerical study of fluid flow and heat transfer in tube banks with stream-wise periodic boundary conditions. *Transactions of the CSME*, **22** (4A) (1998) 397–416.
- [4] P. J. Roache, Perspective: A Method for Uniform Reporting of Grid Refinement Studies. *Journal of Fluids Engineering*, **116** (3) (1994) 405.
- [5] Z. Khalifa, L. Pocher, N. Tilton, Regimes of flow through cylinder arrays subject to steady pressure gradients. *International Journal of Heat and Mass Transfer*, **159** (2020) 120072.
- [6] H. Schlichting, K. Gersten, Boundary-Layer Theory, Springer Berlin Heidelberg, Berlin, Heidelberg (2017).
- [7] S. Meinicke, K. Dubil, T. Wetzel, B. Dietrich, Characterization of heat transfer in consolidated, highly porous media using a hybrid-scale CFD approach. *International Journal of Heat and Mass Transfer*, **149** (2020) 119201.
- [8] V. Gnielinski, Gleichungen zur Berechnung des Wärmeübergangs in querdurchströmten einzelnen Rohrreihen und Rohrbündeln. *Forschung im Ingenieurwesen A*, **44** (1) (1978) 15–25.
- [9] A. Žukauskas, Heat transfer from tubes in crossflow, In: *Advances in heat transfer*, Amsterdam, Elsevier (1972) 93–160.
- [10] A. J. Fowler, A. Bejan, Forced convection in banks of inclined cylinders at low Reynolds numbers. *International Journal of Heat and Fluid Flow*, **15** (2) (1994) 90–99.